npg

Abnormal Indices of Cell Cycle Activity in Schizophrenia and their Potential Association with Oligodendrocytes

Pavel Katsel*[,1], Kenneth L Davis[1], Celeste Li[1], Weilun Tan[1], Elizabeth Greenstein[1], Lisa B Kleiner Hoffman[1] and Vahram Haroutunian[1,2]

[1]Department of Psychiatry, The Mount Sinai School of Medicine, New York, NY, USA; and [2]JJ Peters VA Medical Center, Bronx, NY, USA

The goal of this study was to determine what signaling pathways may elicit myelin-specific gene expression deficits in schizophrenia (SZ). Microarray analyses indicated that genes associated with canonical cell cycle pathways were significantly affected in the anterior cingulate gyrus (ACG), the region exhibiting the most profound myelin-specific gene expression changes, in persons with SZ ($N = 16$) as compared with controls ($N = 19$). Detected gene expression changes of key regulators of G1/S phase transition and genes central to oligodendrocyte differentiation were validated using qPCR in the ACG in an independent cohort (Ns = 45/34). The relative abundance of phosphorylated retinoblastoma protein (pRb) was increased in the white matter underlying the ACG in SZ subjects (Ns = 12). The upregulation of cyclin D1 gene expression and the downregulation of p57[Kip2], accompanied by increased cyclin D/CDK4-dependent phosphorylation of pRb, acting as a checkpoint for G1/S phase transition, suggest abnormal cell cycle re-entry in postmitotic oligodendrocytes in SZ. Furthermore, gene expression profiling of brain samples from myelin mutant animal models, quaking and myelin-associated glycoprotein (MAG) null mice, showed that cell cycle gene expression changes were not a necessary consequence of the reduced gene expression of structural myelin proteins, such as MAG. While, quaking, a known modulator of cell cycle activity during oligodendrocyte differentiation impairs the expression of multiple myelin genes, including those that are affected in SZ. These data suggest that the normal patterns of cell cycle gene and protein expression are disrupted in SZ and that this disruption may contribute to the oligodendroglial deficits observed in SZ.
Neuropsychopharmacology (2008) **33,** 2993–3009; doi:10.1038/npp.2008.19; published online 5 March 2008

INTRODUCTION

Disconnection or aberrant communication among different brain regions is believed to contribute to the abnormal functioning of neural networks and has been postulated to be central to the pathophysiology of SZ (Weinberger, 1995; Friston and Frith, 1995; Weinberger and Lipska, 1995; Arnold and Trojanowski, 1996; Raedler *et al*, 1998; Haroutunian and Davis, 2000; Davis *et al*, 2003). The neurobiological substrates of these connectivity and communication abnormalities remain unknown, but recent evidence suggests that abnormalities in myelination and altered oligodendrocyte (OLG) number and function may be prominent contributors to SZ.

Historically, myelination has been viewed as a central process supporting the functional synchrony of neural networks. For example, loss of a single myelinating oligodendrocyte may affect the speed of signal conduction and propagation (Baumann and Pham-Dinh, 2001) in as many as 40 axons (Larocca and Rodriguez-Gabin, 2002). Thus, abnormalities in a single oligodendrocyte can be amplified to affect signaling in multiple neurons. In addition, recent animal model studies have implicated OLG involvement in modulating neurotransmission and thus may contribute to disturbances in neurotransmission that are associated with SZ (Roy *et al*, 2007). For example, OLGs play a significant role not only in regulating glutamate function (Gallo and Ghiani, 2000), but the downregulation of OLG-associated genes has also been shown to affect the levels and metabolism of dopamine in rodent models (Nikulina *et al*, 1995; Roy *et al*, 2007). In addition, OLG-specific gene expression abnormalities in animals can significantly influence neurotransmission, signal conduction, behavior, and neuronal morphology in ways that resemble some of the abnormalities noted in SZ (Benes *et al*, 1986; Rajkowska *et al*, 1998; Selemon *et al*, 1998; Roy *et al*, 2007). Finally, there is an apparent temporal relationship between myelination and the onset of SZ. Myelination in the frontal and temporal lobes, brain regions consistently implicated in the pathophysiology of SZ, occurs during late adolescence to early adulthood corresponding

*Correspondence: Dr P Katsel, Department of Psychiatry, Room 4F-20, JJ Peters VA Medical Center, Research Build. (151), 130 West Kingsbridge Road, Bronx, NY 10468, USA, Tel: + 1 718 584 9000 ext 6067, Fax: + 1 718 365 9622, E-mail: pavel.katsel@mssm.edu
Received 13 November 2007; revised 23 January 2008; accepted 24 January 2008

closely to the peak incidence of SZ onset (Huttenlocher, 1979; Terry et al, 1987; Benes, 1989; Benes et al, 1994; Goldman-Rakic and Selemon, 1997; Giedd et al, 1999). Thus, myelin gene expression abnormalities may have consequences for chemo- and cyto-architectural organizations that are consistent not only with some of the most robust neurobiological findings in SZ, but also with the disconnectivity hypothesis in SZ (Friston and Frith, 1995; Weinberger and Lipska, 1995).

Neuropathological studies in SZ have identified abnormalities in portions of the limbic system and its associated circuits (prefrontal cortex, cingulate, temporal gyri, and hippocampus) that are thought to subserve many of the aberrant behavioral and psychotic symptoms of SZ (Stevens, 1973; Torrey and Peterson, 1974; Kovelman and Scheibel, 1984; Barta et al, 1990; Rajkowska et al, 1998; Selemon et al, 1998; Selemon and Goldman-Rakic, 1999; Benes, 1999; Goldman-Rakic, 1999; Lim et al, 1999; Harrison, 1999; Weinberger, 1999; Haroutunian and Davis, 2000; Tamminga et al, 2000; Benes et al, 2001; Meyer-Lindenberg et al, 2001; Selemon and Rajkowska, 2003). These observations of multi-regional abnormalities have not been limited to neurons, as morphometric studies have shown reductions in glial cell densities in the anterior cingulate cortex (Cotter et al, 2001; Stark et al, 2004) as well as layer-specific reductions of glia in the dorsolateral prefrontal cortex of persons with SZ (Rajkowska et al, 2002; Hof et al, 2003). Adult myelinating OLGs are terminally differentiated postmitotic glial cells generated during early development from multipotent glial progenitor cells (OPC) (Liu et al, 2002). Evidence for the involvement of OLGs and myelin in the pathophysiology of SZ has come from analysis of postmortem tissue from persons with SZ using protein (Flynn et al, 2003; Dracheva et al, 2006) and gene expression studies (Hakak et al, 2001; Bahn and Jones, 2003; Tkachev et al, 2003; Aston et al, 2004; Iwamoto et al, 2005; Katsel et al, 2005a, b; Dracheva et al, 2006), light and electron microscopic studies (Miyakawa et al, 1972; Uranova et al, 2001, 2004; Vostrikov et al, 2007), and in vivo neuroimaging studies (Buchsbaum et al, 1998; Lim et al, 1999; Foong et al, 2000; Foong et al, 2001; Bartzokis et al, 2003). Recent gene expression studies have extended previous reports of myelin-associated gene expression deficits in the frontal cortex in SZ (Hakak et al, 2001; Bahn and Jones, 2003; Tkachev et al, 2003; Katsel et al, 2004, 2005b; Sugai et al, 2004; Iwamoto et al, 2005; Aberg et al, 2006a) to suggest that the cingulate cortex and the hippocampus are regions of special vulnerability (Katsel et al, 2005a, b; Dracheva et al, 2006). Although one recent post mortem gene and protein expression study failed to validate changes for four myelin-specific genes in DLPFC of persons with SZ (Mitkus et al, 2008). The human quaking gene (QKI), which encodes four major differentially spliced isoforms, is one of the OLG-associated genes whose expression is significantly affected in SZ (Haroutunian et al, 2006b; Aberg et al, 2006b). QKI has also been implicated in association studies (Aberg et al, 2006b). Current research has shown that downregulation of gene expression of the QKI transcript isoforms in quaking mice can hamper normal OLG differentiation (Larocque et al, 2005) and is suggestive of intrinsic unsuppressed cell cycle activity in OLGs of quaking mice.

In the canonical view of cell cycle regulation of somatic cells, mitogens, and/or growth factors elicit increases in the cyclins D—family of proteins and the activity of their associated kinases (Cdk4/6) and sequester the Cip/Kip family of Cdk inhibitors (p21^{Cip1}, p27^{Kip1}, and p57^{Kip2}). Both proteins are believed to be the initial steps in the progression of cell cycle (G1/S phase transition). The activity of the CCND/Cdk4/6 complexes results in phosphorylation of the retinoblastoma (pRb, p107, and p130) family of 'pocket' proteins. Dephosphorylated pRb acts as a suppressor of cell cycle progression. Phosphorylation of pRb, mediated by serine/threonine cyclin-dependent kinases, relieves this proliferation suppression activity and liberates E2F transcription factors. In turn, E2Fs initiate transcription of cell cycle proteins including cyclin E (CCNE) (Geng et al, 1996; Lundberg and Weinberg, 1998). The resulting CCNE/Cdk2 complex accumulation finalizes the G1 to S phase transition by complete inactivation of pRb through its phosphorylation (see cartoon in Figure 7) and coordinates histone synthesis for chromosomal DNA replication (Lundberg and Weinberg, 1998). QKI isoforms 6 and 7 intervene with progenitor cell proliferation by binding and increasing the stability of p27^{Kip1} mRNA, which results in a rise of the p27^{Kip1} protein believed to be a critical step in ensuring cell cycle arrest and subsequent differentiation into mature OLGs (Larocque et al, 2005). The other two Cdk inhibitors, p21^{Cip1} and p57^{Kip2} also play important roles in OLG differentiation. p57^{Kip2} is an important component of the intrinsic molecular timer that regulates the number of divisions in OPC before the onset of differentiation. p21^{Cip1} is necessary for OLG differentiation, but not necessarily for cell cycle arrest (Dugas et al, 2007).

We hypothesized that the widespread OLGs/myelin abnormalities observed in SZ may be due to events associated with the proliferation and differentiation of OLGs. This hypothesis is supported in part by the in situ and genetic evidence for the involvement of QKI in SZ. In the studies described here, we have focused on canonical cell cycle pathways by analyzing postmortem gene expression profiles in the ACG of persons with SZ and control subjects using Affymetrix's GeneChip® based microarray technology. We have validated the microarray findings by qPCR and protein analysis in independent samples. In addition, we have found that OLG-related cell cycle abnormalities may underlie the wide spread myelin deficits in some animal models with OLG-specific mutant genes providing further insights into the potential neurobiological mechanisms of OLG-associated deficits in SZ.

MATERIALS AND METHODS

Sample Information and Preparation of Total RNA

Brain tissue specimens were derived from the Brain Bank of the Department of Psychiatry of the Mount Sinai School of Medicine (New York, NY)/JJ Peters VA Medical Center (Bronx, NY). The precise tissue handling procedures have been described in detail (Haroutunian et al, 1998, 1999, 2006a, 2007; Davis et al, 1999). Controls were derived from nursing home residents who, on extensive medical chart review and care-giver interview, evidenced no neurological or neuropsychiatric diseases and died of natural causes

(myocardial infarction, various nonbrain nonhepatic cancers, and congestive heart failure). All brain specimens were examined in detail by board certified neuropathologists using standardized procedures (Mirra et al, 1991). Specimens from any SZ or control cases that evidenced any discernable neuropathology were excluded from study (Purohit et al, 1998). None of the cases or controls had any history of licit or illicit drug abuse (tobacco use excepted).

Fourteen cerebral cortical regions (BAs: 8, 10, 44, 46, 4, 23/31, 24/32, 20, 21, 22, 36/28, 38, 7, 17) and the hippocampus were dissected from flash frozen coronal sections, pulverized at -80°C and aliquoted. Anterior cingulate (ACG, BA: 24/32) were dissected at the level of the genu of the corpus callosum. Aliquots (50 mg) from each region were used for microarray gene expression analysis. Total RNA isolation and preparation for the microarrays were as described previously (Katsel et al, 2005a, b). Similarly prepared aliquots from the ACG and the white matter underlying the ACG were used in qPCR and western blot analyses (Dracheva et al, 2006; Haroutunian et al, 2006b).

All subjects died of natural causes with no history of licit or illicit drug abuse or neurological disease. Patients were diagnosed antemortem according to the Diagnostic and Statistical Manual of Mental Disorders, Fourth Edition criteria as described (Dracheva et al, 2005). Control (CNT) subjects (nursing home residents) with no evidence of neurological or neuropsychiatric diseases were matched with SZ subjects by age, postmortem interval (PMI), and brain pH (Table 1). Diagnostic and postmortem consent procedures were approved by the institutional review boards of Mount Sinai, Bronx VA, and Pilgrim Psychiatric Center.

A larger and independent set of brain tissue specimens from anterior cingulate (ACG, BA: 24/32—at the level of the genu of the corpus callosum) was used for the qPCR experiments (Table 1). Mean RNA integrity numbers for control samples were 7.22 ± 0.99 and 7.16 ± 1.34 for SZ group. Ten of these subjects with SZ had been free of anti-psychotic medication for 4 weeks or more prior to death (Table 1). The half-life of haloperidol in the brain of chronically treated subjects is estimated to be about 6.8 days (Kornhuber et al, 1999). Therefore, after four or more half-lives of haloperidol, the brains of these subjects should have retained only a residual amount of the drug. Specimens from these cases were used in subgroup analyses to determine the effects of anti-psychotic medication.

Animal Maintenance and Samples

Brains of quaking-qk^{e5} homozygous mice were gifts of Dr Monica J Justice (Baylor College of Medicine, Houston, TX). The qk^{e5} mutation was induced on 101/R1 DNA after treatment with N-ethyl-N-nitrosourea and maintained as described previously (Noveroske et al, 2005). The molecular defect in the qk^{e5} allele is not known, but protein expression studies have shown decreased expression QKI-5 and lack of QKI-6 and -7 isoforms in postnatal OLGs (Noveroske et al, 2005). Myelin-associated glycoprotein (MAG) null mutant mice (Mag^tm1Rod strain, Jackson Laboratory, Bar Harbor, ME) were maintained by sibling mating.

Genotypes were distinguished by PCR using conditions as outlined in the Jackson Laboratory protocol. Two to three-month-old qk^{e5} mice with corresponding background wild type ($N = 4$/group) and 6–12 month old MAG null mice with corresponding background wild type ($N = 8$/group) were used in the study. Mice were killed by decapitation and the brains were removed and immediately dissected. Each brain was divided midsagitally. The left halves of the brains were stored at -80°C. The right halves were dissected fresh. Dissections included the frontal cortex gray matter (from the frontal pole to the beginning of the parietal cortex (bregma -1.8 (Franklin and Paxinos, 1997)), the corpus callosum underlying the dissected frontal cortical gray matter, and the hippocampus. The border of the frontal cortex and the parietal cortex was identified as the coronal block where the middle cerebral artery bifurcates from the internal carotid artery (Zeman and Innes, 1963) and the dissections were limited to the cortical region dorsal to the rhinal fissure. Procedures for total RNA isolation and cDNA preparation for qPCR have been described previously (Dracheva et al, 2001).

Microarray Procedure and Data Analysis

Microarray analysis was performed using Affymetrix (Santa Clara, CA) HG-U133AB GeneChip® set as described in the standard protocol outlined in the GeneChip® Expression Analysis Technical Manual (Affymetrix Inc., Santa Clara, CA) and reported previously (Katsel et al, 2005a, b; Haroutunian et al, 2007). Data were normalized using MAS 5.0 algorithms and analyzed using the GX™ Explorer v.3.0 (Gene Logic Inc., Gaithersburg, MD) tools (expression, comparative, and contrast analysis) as described previously (Katsel et al, 2005a, b, c). To reduce false discovery (Type I error), error rate gene expression change was considered to be significantly altered if the change in expression met the

Table 1 Characteristics of the Sample Groups Used in Microarray, qPCR and Protein Studies of ACG

Characteristics	Control (array)	SZ (array)	Control (qPCR)	SZ (qPCR)	Control (western's)	SZ (western's)
Patient number	19	16	34	45	12	12
Sex (M/F)	8/11	13/3	20/17	19/26	7/5	7/5
Age (years)	80.5 ± 12.27	74.3 ± 11.6	79.38 ± 12.24	76.48 ± 10.68	74.7 ± 9.66	81.2 ± 9.66
Brain pH	6.51 ± 0.26	6.46 ± 0.23	6.49 ± 0.25	6.47 ± 0.28	6.52 ± 0.30	6.47 ± 0.29
PMI (min)	462 ± 392	522 ± 423	532 ± 434	826 ± 440	742 ± 462	852 ± 322

Data are expressed as a mean ± SD.

relatively stringent criteria of $p < 0.05$ relative to the expression level in the control group; fold change $\geqslant 1.7$, present calls $\geqslant 80\%$. To validate the results obtained by MAS 5.0 analysis the raw microarray data from 2147 HG-U133A and B individual chips were transformed and analyzed using GeneSpring GX 7.3.1 (Agilent Technologies/Silicon Genetics, Santa Clara, CA). Raw data were prenormalized with Robust Multi-Chip Average (RMA) (Bolstad *et al*, 2003; Irizarry *et al*, 2003) with subsequent log transformation, normalization to the 50th percentile of all values per chip and median-centred per gene using GeneSpring normalization. Statistical comparisons were made using Gene-Spring's Cross Gene Error Model (CGEM), based on the deviation from 1.0 algorithm. To minimize the false positive/negative error rate in these GeneSpring/RMA/CGEM analyses, we used a combination of confidence ($p \leqslant 0.05$) and fold change ($\geqslant 1.6$) with Benjamini and Hochberg multiple testing corrections (Benjamini and Hochberg, 1995). Genes accepted for subsequent validation by qPCR were those that met the high stringency criteria by both MAS 5.0- and RMA-based normalization of microarray analyses.

Ingenuity Pathway Analysis

A dataset containing identifiers for the genes expressed (presence $\geqslant 80\%$) in the samples from the ACG (~ 3580 transcripts) and corresponding *p*-values obtained from the comparison analysis (MAS5.0 normalization, GX™ Explorer v.3.0, Gene Logic Inc.) between control and SZ samples was uploaded into the application. Differentially regulated genes ($p \leqslant 0.05$) were overlaid onto a global molecular network in the Ingenuity Pathways Knowledge Base (Ingenuity® Systems, www.ingenuity.com) to identify biological functions and canonical pathways. Ingenuity pathway analysis algorithmically generates networks of genes based on their connectivity. Fischer's exact test was used to calculate a *p*-value determining the probability that each biological function assigned to that dataset, or the association between genes in the dataset and the canonical pathway, was not due to chance alone. Significant ($ps < 0.05$) canonical pathways were additionally ranked according to the ratios between the numbers of genes from the dataset that mapped to the pathway to the total numbers of genes in the canonical pathway. The scores for the networks were calculated based on the number of network eligible genes and the size of the network to approximate how relevant any particular network was to the total list of eligible genes. Only the top five scoring networks are shown (Table 3).

RT-qPCR

The mRNA levels of myelin and cell cycle genes, which met selection criteria of both MAS 5.0- and RMA-based microarray analysis were measured by qPCR in a larger independent cohort (Table 1) using TaqMan® MGB probes and primer sets (Applied Biosystems, Foster City, CA). CDK inhibitor-p21$^{\text{Cip1}}$, which did not show significant changes in the microarrays, was additionally included for qPCR experiments to test the possibility that all three members of Cip/Kip family of CDK inhibitors are affected in the ACG of persons with SZ. TaqMan® probe ID's for selected cell cycle genes and normalization controls are listed in Table 2.

For relative quantification of mRNA expression, geometric means were calculated using the comparative $2^{-\Delta\Delta C_t}$ method described previously (Dracheva *et al*, 2005). Three housekeeping genes (GUSB, PPIA, and PGK1) were selected for human postmortem studies in ACG after comparison of six different endogenous controls and their analysis for expression stability using geNorm (http://medgen.ugent.be/~jvdesomp/genorm/). Two housekeeping genes (GAPDH and PPIA) were used as the endogenous references in the mouse studies. Microglial-specific marker—CD68 was not expressed abundantly enough in the brain samples examined for reliable analysis.

Quantitative Western Blotting

Protein abundance was measured in the ACG and white matter (underlying the ACG) from SZ and CNT subjects ($N = 12$/group) previously selected for microarray analysis (Table 1) and in brain samples from *qke5* and wild-type mice ($N = 4$/group) using western blotting. To evaluate the stability of the cyclin D/Cdk complex-dependent phosphorylated retinoblastoma protein (pRB) at different postmortem intervals (Figure 3), mouse brain tissue specimens (~ 15 mg) were dissected from the same animals and were immediately frozen or stored for either 6 or 20 h at room temperature before homogenization and western blotting.

Tissue specimens (~ 50 mg-human, ~ 15 mg-mouse) were homogenized in Urea/Tris solution: 50 mM Tris/HCl pH 7.4; 6 M Urea; 2% CHAPS containing 1 mM PMSF and cocktails of proteinase/phosphatase inhibitors (Pierce Biotech Inc., Rockford, IL). Total protein concentration in the tissue homogenates was determined with a CBQCA Quantitation Kit (Molecular Probes Inc., Eugene, OR). Aliquot samples of 15 µg of total protein in triplicates were loaded onto precast 4–12% Tris–glycine gel (Invitrogen, Carlsbad, CA) under reduced conditions. A 'standard calibrator' (a mix of small aliquots of tissue from all samples) was used as a calibrator between the gels and run on each gel in triplicate. Electrophoresis, blotting, immunostaining and detection (ECL Plus-GE Healthcare, Piscataway, NJ) were performed under standard conditions. Mouse monoclonal antibodies: anti-human phosphorylated Ser608 pRB were from AbD/Serotec (Raleigh, NC); anti-mouse phosphorylated Ser807/811 pRB—from Cell Signaling Technology Inc., (Danvers, MA); anti-human dephosphorylated pRb—from BD PharMingen (Franklin Lakes, NJ); total pRB—from Santa Cruz Biotech Inc., (Santa Cruz, CA) and anti-GAPDH was from Biodesign International (Saco, ME). The linearity of the dose responses for the antibodies used was established in preliminary experiments. Film images were digitized on Alpha ChemImager™5500 and quantitated with AlphaEaseFC software (Alpha Innotech Corp, San Leandro, CA). To account for gel to gel variability, the relative expression value of ppRb (Ser608) or ppRb (Ser807/811) in each sample was calculated as a ratio between the averaged intensities of the band in the experimental sample and in the 'standard-calibrator'. The relative abundance of GAPDH and total pRb protein was determined in the same manner as for ppRb. Finally, mean values of the ratios of ppRb/GAPDH and ppRb/total pRb were normalized to the amount of total protein.

Table 2 TaqMan Gene Expression Assays Used in the Study

Gene symbol	Species	AB Assay ID	NCBI accession no	Exon boundary	Location
CCND1	Homo sapiens	Hs00277039_m1	NM_053056.1	Exon 2 | Exon3	625
CCND2	Homo sapiens	Hs00153380_m1	NM_001759.2	Exon3 | Exon4	845
CCNE2	Homo sapiens	Hs00180319_m1	NM_057749.1	Exon 7 | Exon 8	705
CDKN1A (p21^{Cip1})	Homo sapiens	Hs00355782_m1	NM_078467.1	Exon 2 | Exon 3	680
CDKN1B (p27^{Kip1})	Homo sapiens	Hs00153277_m1	NM_004064.2	Exon 1 | Exon2	945
CDKN1C (p57^{Kip2})	Homo sapiens	Hs00175938_m1	NM_000076.1	Exon 1 | Exon2	1080
GUSB	Homo sapiens	Hs99999908_m1	NM_000181.1	Exon 11 | Exon 12	1816
NPAT	Homo sapiens	Hs00159638_m1	NM_002519.1	Exon10 | Exon11	945
PGK1	Homo sapiens	Hs99999906_m1	NM_000291.2	Exon 4 | Exon 5	494
PHB	Homo sapiens	Hs00855044_g1	NM_002634.2	Exon 7 | Exon 7	1263
PPIA	Homo sapiens	Hs99999904_m1	NM_021130.3	—	435
RBL2	Homo sapiens	Hs00180562_m1	NM_005611.2	Exon 8 | Exon 9	1250
TFDP1	Homo sapiens	Hs00955491_gH	NM_007111.3	Exon 6 | Exon 7	682
CCND1	Mus musculus	Mm00432359_m1	NM_007631.1	Exon 3 | Exon 4	714
CCND2	Mus musculus	Mm00438071_m1	NM_009829.3	—	680
CDKN1A (p21^{Cip1})	Mus musculus	Mm00432448_m1	NM_007669.2	Exon 2 | Exon 3	525
CDKN1B (p27^{Kip1})	Mus musculus	Mm00438168_m1	U10440.1	Exon 2 | Exon 3	819
CDKN1C (p57^{Kip2})	Mus musculus	Mm00438170_m1	NM_009876.2	Exon 2 | Exon 3	1028
CNP1	Mus musculus	Mm01306640_m1	NM_009923	—	759
GAPDH	Mus musculus	Mm99999915_g1	NM_001001303.1	Exon 2 | Exon 3	—
MAG	Mus musculus	Mm00487538_m1	NM_010758	Exon 5 I Exon 6	558
MBP	Mus musculus	Mm00521979_m1	NM_010777	—	436
PLP1	Mus musculus	Mm01297210_m1	NM_011123	Exon 2 | Exon 3	340
PPIA	Mus musculus	Mm02342429_g1	NM_008907.1	Exon 3 | Exon 4	—
QKI	Mus musculus	Mm00498991_m1	NM_021881	Exon 4 | Exon 5	1190

Statistical Data Analysis

Multiple statistical procedures were employed for different aspects of the study. Max t-scores (Budhraja et al, 2003; Mariani et al, 2003) for each individual transcript were calculated by contrast analysis of MAS5.0 normalized microarray data using GX™ Explorer v.3.0 (Gene Logic Inc., Gaithersburg, MD). t-scores were used as a standardized measure of gene expression change for each individual transcript across all of the analyzed brain regions as described previously (Katsel et al, 2005b, 2007). The calculation algorithm of t-scores takes into account variability across all studies brain regions. Accordingly genes with high magnitudes of changes and lower variability have higher t-scores than those with similar mean changes but high variability. Differences in expression between CNT and SZs in the ACG in the GeneSpring/RMA/CGEM analyses were examined using a one-way analysis of variance (ANOVA) with Benjamini and Hochberg multiple testing corrections (Benjamini and Hochberg, 1995).

Consistent with previously published procedures (Katsel et al, 2005b) categorizations by gene ontology (GO) was based on functional class scoring (FCS) (Pavlidis et al, 2002, 2004) which examines the statistical distribution of individual gene scores (t-scores) for each gene among all genes in the GO class. FCS was carried out by the ErmineJ software (ver. 2.1.12, University of British Columbia, Vancouver) on the complete list of transcripts with detection p-values $\leqslant 0.06$

(13 472 transcripts) without any additional selection criteria. GO terms were only considered if between eight to 150 unique members were assayed for that class.

Correlations were performed based on cell cycle gene expression changes from the microarray data to determine their association with any particular neural cell population. For correlations, individual intensity values (MAS5.0 normalized) of five cell cycle genes (cyclins D1, D2, E2, and CDK inhibitors, p27^{Kip1} and p57^{Kip2}), two myelin/OLG-specific markers (PMP22 and SOX10), one astrocyte (GFAP) and two neuronal markers (MAP2 and NEFL) were selected (Table 5) from ACG and analyzed. A two-tailed Student's t-test was used to compare relative mRNA expression of cell cycle and myelin/OLG-specific genes in qPCR experiments and relative abundance of ppRb protein in human and animal models experiments. Student's t-test and correlation analyses were performed using Statistica (release 6.0).

RESULTS

Canonical Cell Cycle Pathways Affected in SZ as Revealed by Microarray Analysis

We have shown in previous studies (Katsel et al, 2005b; Haroutunian et al, 2006b) that the ACG is one of the four regions (BAs 23/31, 24/32, 21, and HIPP) where alterations in the expression of OLG/myelin genes are most prevalent

in SZ. In those studies, multiple gene ontology categories, related to myelination/nerve ensheathment, contributed to nearly half of the top 20 Gene Ontology categories in the cingulate gyri of persons with SZ (Katsel *et al*, 2005b). Ingenuity Pathway Analysis was used to reanalyze those results and determine what signaling pathways were affected in the ACG of persons with SZ. Cell cycle or cell cycle-related categories represented by highly significant *p*-values (Fischer's test) were at the top of the list of gene networks, molecular/cellular functions and potential disorders that were affected in the ACG in SZ (Table 3). Cell cycle-related function appeared to be associated with three of the top five gene networks. Additionally, cell cycle canonical pathways, including G1/S checkpoint regulation and G2/M DNA damage checkpoint regulation were among the significantly affected canonical pathways in the ACG of persons with SZ. We additionally analyzed differentially expressed genes in the ACG by the FCS method to test whether cell cycle-related categories maintain significance after multiple testing (200 000 iterations) against randomly generated gene classes of the same size. The *p*-values of categories related to cell cycle (mitosis, G1/S phase, and M phase of mitotic cell cycle) remained highly significant ($p < 0.001$).

Microarray data (contrast analysis *t*-scores (Katsel *et al*, 2005b)) from both ACG and from all of the brain regions examined, implicated two members of the cyclins D family, CCND1 and CCND2, the main activators of the G1 phase entry. These two genes were among the top 10 cell cycle genes upregulated in SZ (Table 4). On the other hand, genes that are critical to cell cycle inhibition, p27^{Kip1}, p57^{Kip2}—inhibitors of the CCND/CDK4,6 complexes—were downregulated, suggesting activation of the cell cycle and transition from G1 to S phases (Table 4). Upregulation of the genes associated with the S phase of the cell cycle, ORC5 L, MCM3, and CDK6 (Table 4), suggests further that DNA replication may also be in an active state in SZ. Overall, detected cell cycle genes (Table 4) remained within the top 15% of all differentially expressed genes across all of the 15 brain regions, or within the top 5% of differentially expressed genes in ACG.

RMA-CGEM methods using ANOVA with Benjamini Hochberg multiple testing corrections confirmed the five differentially expressed genes in SZ cell cycle (p27^{Kip1}, p57^{Kip2}, CCND1, CCND2, CCNE2, *p*s < 0.05) that met MAS5.0 stringency criteria (Table 4). In addition, RMA-CGEM analysis using ANOVA with Benjamini Hochberg multiple testing corrections revealed the differential expression of four other genes integral to G1/S phase checkpoint progression. These included the upregulated transcription factor DP1 (TFDP1, $p = 0.0004$), the nuclear protein ataxia-telangiectasia locus (NPAT, $p = 0.002$), the downregulated retinoblastoma like 2 (RBL2, $p = 0.0001$) and prohibitin (PHB, $p = 0.009$).

Majority of Complex Correlations Between Gene Expression of Cell Cycle Proteins and Neuronal or Glial Markers in Controls are Absent in SZ

Correlations between mRNA levels of cell cycle genes and established cell-specific markers/genes were performed to determine whether the expression of the identified cell cycle

Table 3 Summary of Ingenuity Pathway Analysis

	Top networks	
Number	**Associated network functions**	**Score**
I	Cellular development, cellular growth and proliferation, nervous system development	39
2	RNA post-transcriptional modification, gene expression, molecular transport	37
3	Cell cycle, embryonic development, tissue development	37
4	Cancer, reproductive system disease, renal, and urological disease	37
5	Gene expression, viral function, cellular compromise	37

	Top functions	
Disease and disorders	***p*-value**	**Number of molecules**
Cancer	0.0007–0.04	54
Neurological disease	0.001–0.04	I9

	Molecular and cellular functions	
Cell cycle	0.0004–0.04	49
Cell to cell signaling and interaction	0.0007–0.04	43
Lipid metabolism	0.002–0.04	52
Molecular transport	0.002–0.04	62
Small molecule biochemistry	0.002–0.04	8I

genes was associated with any particular neural cell population. Correlation coefficients between five cell cycle genes, two myelin/OLG, two neuronal markers and one marker for astrocytes are shown (Table 5).

In controls, the RNA expression levels of the CDK inhibitors, p27^{Kip1} and p57^{Kip2} were positively correlated with each other and with cyclin E2, and were negatively correlated with cyclin D2 (*p*s < 0.01). The glial and neuronal markers showed significant positive correlations within their cell type-specific groups and negative correlations between cell type-specific groups indicating marker specificity (*p*s < 0.05). When tested against cell-specific markers, most of the tested cell cycle genes demonstrated complex but predictable relationships with OLG, astrocytic, and neuronal markers. CDK inhibitors, p27^{Kip1}, p57^{Kip2}, and cyclins E2, and D1 exhibited positive correlations with OLGs markers (*p*s < 0.05), and negative correlations with neuronal markers (*p*s < 0.05). In contrast, CCND2 showed negative correlations with OLG markers, but positive correlations with the expression of genes encoding neuronal proteins (*p*s < 0.05). Additionally, the astrocyte marker, glial fibrillary acidic protein (GFAP), was positively correlated with p57^{Kip2} and negatively correlated with CCND2 (*p*s < 0.05). The majority of these correlations remained

Table 4 Differentially Expressed Cell Cycle Genes in 15 Brain Regions in SZ

Gene name	Symbol	t-score
Upregulated		
Cyclin D2	CCND2	4.69
Origin recognition complex, subunit 5-like	ORC5L	4.37
Histone deacetylase 8	HDAC8	3.36
Transforming growth factor, β 3	TGFB3	3.30
Cyclin D1	CCND1	3.18
MAD2 mitotic arrest deficient-like 1	MAD2L1	2.89
SMAD, mothers against DPP homolog 3	SMAD3	2.63
Cyclin-dependent kinase 6	CDK6	1.62
Downregulated		
Growth arrest and DNA-damage-inducible, β	GADD45B	−7.93
Growth arrest and DNA-damage-inducible, α	GADD45A	−6.46
Cyclin-dependent kinase inhibitor 1C (p57^{Kip2})	CDKN1C	−5.55
Cyclin-dependent kinase inhibitor 1B (p27^{Kip1})	CDKN1B	−4.95
Budding uninhibited by benzimidazoles 3 homolog (yeast)	BUB3	−4.89
Proliferating cell nuclear antigen	PCNA	−4.83
Cell division cycle 14 homolog B	CDC14B	−4.62
Structural maintenance of chromosomes 1-like 1	SMC1L1	−4.21
Retinoblastoma protein 1	RB1	−2.64

The *t*-scores were calculated by contrast analysis (GX^{TM} Explorer v.3.0, Gene Logic Inc.) as described previously (Katsel *et al*, 2005a, b), Genes are arranged in descending order or magnitude of change.

significant even after Bonferroni correction for multiple tests of significance.

When the expression values for the same cell cycle genes and cell-specific marker/genes were compared in the SZ samples, only three cell cycle genes were significantly correlated with OLG markers (p27^{Kip1} and p57^{Kip2} were positively correlated and CCND2 was negatively correlated) ($ps < 0.05$), and one gene, p27^{Kip1} was negatively correlated with the MAP2 neuronal marker ($r = -0.53$; $p = 0.04$). As for cell-specific marker/genes, the statistically significant negative correlations between neurons and glia observed in controls were entirely lost in SZ samples, suggesting disassociation of transcription profiles for the expression of the measured genes in neurons and glia in SZ. In contrast, CCND1 which did not exhibit significant correlations with the astrocyte marker, GFAP, in controls showed significant positive correlations with GFAP in SZ.

Real-Time PCR Validation of Alterations in Gene Expression of Key G1/S Phase Checkpoint Proteins

Ten cell cycle genes (Table 6) that met high stringency filtering conditions by the two different microarray

normalization methods (MAS5.0 and RMA-CGEM) were selected from the list of differentially expressed genes in SZ for qPCR analysis in an independent and significantly larger sample of cases and controls from the ACG.

As shown in Figure 1 the expression of p57^{Kip2} was lower in SZs and the relative expression of cyclin D1, TFDP1, and NPAT was higher in SZs relative to controls. Table 6 lists fold changes and significant values (*t*-test) between relative expression of the 10 cell cycle genes in SZ and control samples from ACG. Together, fold change ratios and significant *p*-values indicated strong gene expression changes for CCND1, TFDP1, NPAT, and p57^{Kip2} in ACG in SZ. Sample pH, PMI or age of the donors did not correlated significantly with gene expression levels, except for p57^{Kip2} which showed negative correlation with PMI ($r = -0.43$, $p = 0.001$).

The qPCR showed that gene expression changes for four validated cell cycle genes (Figure 1 and Table 6) were even more pronounced in the subgroup of patients who had been free of anti-psychotic medication for 4 weeks or more prior to death (SZ$_{OFF}$), as supported by the increased magnitude of the fold change ratios (Table 6). Non-affected cell cycle proteins—p21^{Cip1}, p27^{Kip1}, CCND2, RBL2, CCNE2, and PHB remained unchanged in the SZ$_{OFF}$ subgroup.

Increased Phosphorylation of Retinoblastoma Protein in the White Matter and ACG in SZ and Quaking Mice

Based on the multiple lines of evidence supporting abnormal OLG differentiation in quaking mice (Larocque *et al*, 2005) and possible unsuppressed cell cycle activity in OLGs, we assessed the possibility of increased phosphorylation of pRb in the white matter of quaking mice as compared to wild-type mice. As shown in Figure 2 phosphorylation of pRb at S807/811 was significantly increased ($p = 0.002$) in the white matter of quaking mice.

The relative abundance of ppRb (S807/811) at different postmortem intervals in mouse brain, reflecting stability of the cyclin D/Cdk complex-dependent phosphorylation of pRb, is shown in Figure 3. The ppRb band showed an initial $\sim 27\%$ decrease in relative intensity values during the first 6 h postmortem at room temperature, but remained constant thereafter for up to 20 h at room temperature. This observation suggests that postmortem interval should not profoundly impact or falsely inflate the levels of phosphorylated pRb in the closely matching human specimens.

Phosphorylation at the S608 of pRb, distinctive for phosphorylation by either cyclin D1/CDK4 or cyclin A/CDK2 complexes, but not by the cyclin E/CDK2 kinase complex (Zarkowska and Mittnacht, 1997), was significantly ($p = 0.024$) increased in the white matter and demonstrated a tendency to increase in the ACG gray matter of subjects with SZ relative to controls (Figure 4).

Alterations in Gene Expression of Cell Cycle Proteins in Myelin Mutant Mice Models

These studies sought to determine whether cell cycle gene expression changes accompany gene expression deficits in OLG/myelin genes in mouse models systems that are reminiscent of those in ACG of subjects with SZ. Gene

Table 5 Correlation coefficients among the mRNA levels of the cell cycle genes and cell-specific markers in the ACG

	p27^{Kip1} CDKN1B	p57^{Kip2} CDKN1C	Cyclin D1	Cyclin D2	Cyclin E2	MYELIN SOX10	MYELIN PMP22	ASTRO GFAP	NEURON MAP2	NEURON NEFL
p27^{Kip1} CDKN1B		0.2744 p=0.322	0.1904 p=0.497	−0.0660 p=0.815	*0.6148* *p=0.015*	*0.6567* *p=0.008*	0.4478 p=0.094	−0.1758 p=0.531	*−0.5335* *p=0.041*	0.3295 p=0.230
p57^{Kip2} CDKN1C	*0.7542* *p=0.000*		0.0638 p=0.821	−0.3525 p=0.198	0.2140 p=0.444	*0.6485* *p=0.009*	*0.6001* *p=0.018*	0.1411 p=0.616	−0.1013 p=0.719	−0.0945 p=0.738
Cyclin D1	0.3421 p=0.179	0.4643 p=0.060		−0.3201 p=0.245	0.4633 p=0.082	0.1302 p=0.644	0.1761 p=0.530	*0.6606* *p=0.007*	−0.2271 p=0.416	0.4734 p=0.075
Cyclin D2	*−0.6543* *p=0.004*	*−0.6582* *p=0.004*	−0.1659 p=0.525		−0.2667 p=0.337	−0.4554 p=0.088	*−0.5278* *p=0.043*	−0.2779 p=0.316	−0.0089 p=0.975	−0.0621 p=0.826
Cyclin E2	*0.6117* *p=0.009*	0.4605 p=0.063	0.3521 p=0.166	*−0.5655* *p=0.018*		0.3948 p=0.145	0.1418 p=0.614	−0.0277 p=0.922	−0.1262 p=0.654	0.3605 p=0.187
MYELIN SOX10	*0.6166* *p=0.008*	*0.8250* *p=0.000*	*0.4919* *p=0.045*	*−0.5614* *p=0.019*	*0.5863* *p=0.013*		*0.9061* *p=0.000*	0.2235 p=0.423	−0.4238 p=0.115	−0.1485 p=0.597
MYELIN PMP22	*0.6613* *p=0.004*	*0.7304* *p=0.001*	0.1640 p=0.529	*−0.7098* *p=0.001*	*0.5680* *p=0.017*	*0.5823* *p=0.014*		0.4170 p=0.122	−0.4443 p=0.097	−0.1909 p=0.496
ASTRO GFAP	0.3552 p=0.162	*0.4939* *p=0.044*	0.4683 p=0.058	*−0.5539* *p=0.021*	0.4168 p=0.096	*0.5337* *p=0.027*	*0.6369* *p=0.006*		−0.2696 p=0.331	0.4813 p=0.069
NEURON MAP2	*−0.6287* *p=0.007*	*−0.7293* *p=0.001*	*−0.6069* *p=0.010*	*0.5402* *p=0.025*	*−0.4985* *p=0.042*	*−0.7885* *p=0.000*	*−0.5383* *p=0.026*	*−0.6784* *p=0.003*		−0.1792 p=0.523
NEURON NEFL	−0.4560 p=0.066	*−0.6363* *p=0.006*	−0.4294 p=0.085	*0.6462* *p=0.005*	*−0.5930* *p=0.012*	*−0.6807* *p=0.003*	*−0.6562* *p=0.004*	*−0.5990* *p=0.011*	*0.6059* *p=0.010*	

Correlation coefficients are presented for the controls (N = 19) in the lower left corner (white cells) and SZs (N = 16)—in the upper right corner (gray cells). Statistically significant correlations are highlighted in bold italic: positive-in red; negative-in blue.

Table 6 Expression analysis of the cell cycle genes in ACG

Gene symbol	SZ$_{total}$ FC ratio	SZ$_{total}$ *p*-value	SZ$_{OFF}$ FC ratio	SZ$_{OFF}$ *p*-value
CCND1	**1.5**	**0.033**	**1.92**	**0.005**
NPAT	**1.2**	**0.005**	**1.34**	**0.003**
TFDP1	**1.35**	**0.011**	**1.5**	**0.01**
p27^{Kip1}	1.18	*ns*	1.07	*ns*
CCNE2	1.03	*ns*	1.01	*ns*
RBL2	−1.02	*ns*	−1.06	*ns*
CCND2	−1.08	*ns*	1.06	*ns*
PHB	−1.12	*ns*	−1.17	*ns*
p21^{Cip1}	−1.11	*ns*	1.36	*ns*
p57^{Kip2}	**−1.47**	**0.039**	**−1.73**	**0.031**

Tissue samples from the ACG of controls ($N = 34$) and SZ ($N = 45$) were analyzed by qPCR. FC Ratio—fold change ratios represent the ratio of geometric means for each gene to the three housekeeping genes in SZ/control (+) and in control/SZ (−) values. SZ$_{total}$—all the subjects with SZ. SZ$_{OFF}$ ($N = 10$)-subjects with SZ, whose neuroleptic treatment was discontinued for at least 4 weeks prior to death. Differentially changed genes ($p < 0.05$) are highlighted in bold. *ns*-non-significant.
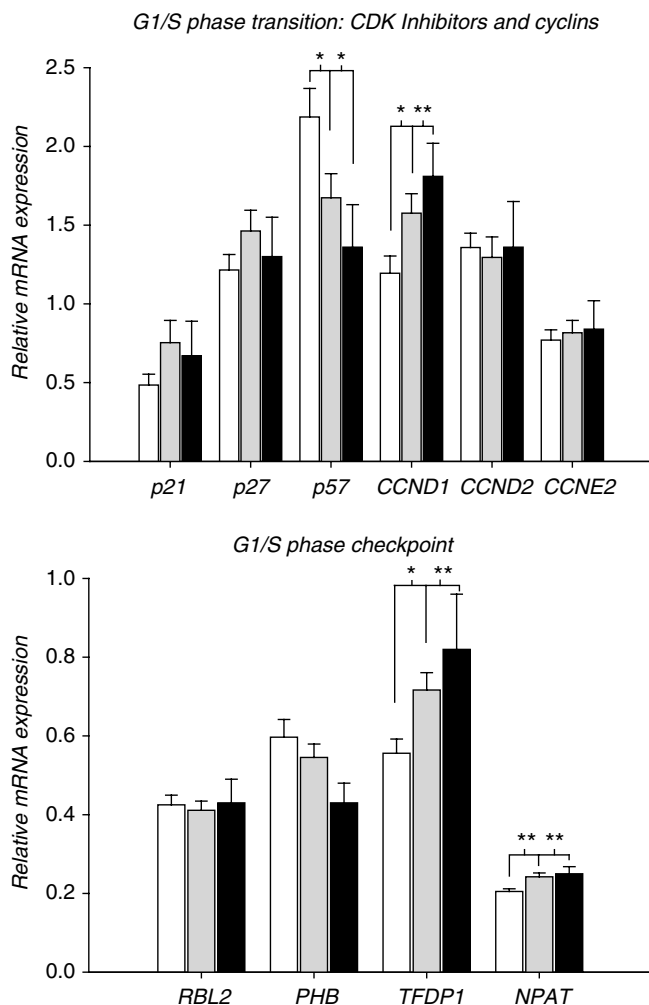
Figure 1 Relative mRNA expression of the G1/S phase checkpoint genes in the anterior cingulate gyrus (BA 24/32) of persons with SZ measured by qPCR. Comparison subjects—white bars ($N = 34$); SZ subjects—gray filled bars ($N = 45$) and SZ$_{OFF}$ subjects whose neuroleptic treatment was discontinued for at least 4 weeks prior to death—black bars ($N = 10$). Data is expressed as geometric means ± SEM of individual expression values normalized to the three housekeeping genes: GUSB, PPIA, and PGK1 as described in Methods.*$ps \leqslant 0.05$; **$p \leqslant 0.01$.
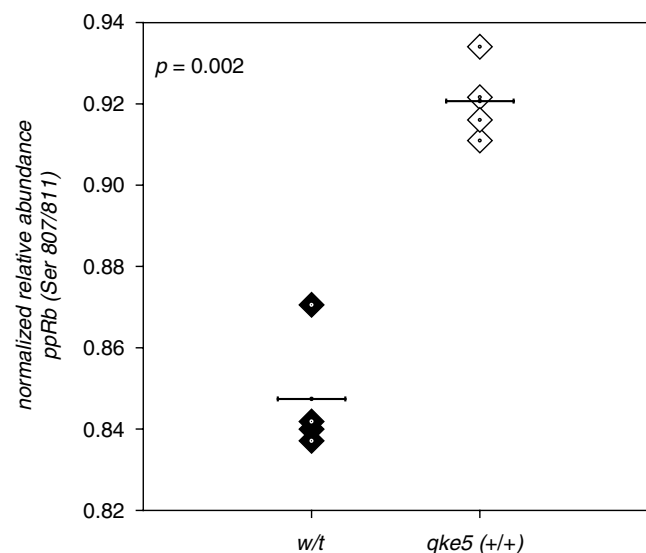

Figure 2 Relative abundance of phosphorylated (S807/811) retinoblastoma protein in the white matter of qk^{e5} mice. Expression of ppRb (S807/811) was measured by western blot. Data expressed as means of ppRb (S807/811) ODs normalized to total pRb/GAPDH and total protein ($N = 4$/group). Plot displays the group means (horizontal line).

expression of a panel of OLG/myelin genes, including MAG, MBP, PLP1, CNP, QKI (the pan probe for all QKI isoform) and a panel of five cell cycle genes including p21^{Cip1}, p27^{Kip1}, p57^{Kip2}, cyclin D1, and D2 was measured by qPCR in the white matter and hippocampus of quaking mice (Figure 5) to determine whether cell cycle gene expression changes accompany gene expression deficits of the OLG/myelin genes. All measured OLG/myelin genes showed significant decreases ($ps \leqslant 0.05$) in the white matter and hippocampus of quaking mice as compared with controls (MAG, CNP, PLP1, and MBP (Figure 5a and b; inserts) and QKI (Figure 5a and b). The gene expression of cyclin D1 and D2 and two CDK inhibitors (p21^{Cip1} and p27^{Kip1}) was decreased ($ps < 0.05$) in both white matter and hippocampus and the expression levels of p57^{Kip2} and cyclin D2 were decreased ($ps < 0.05$) in the white matter of quaking mice (Figure 5, upper panel).

To address the question of whether deficiency of gene expression of a protein important for myelin structural integrity can affect gene expression abnormalities of the canonical cell cycle proteins, gene expression of the same panel of OLG/myelin and cell cycle was measured by qPCR in MAG null mutant mice (Figure 6). In contrast to quaking mice, MAG null mice evidenced significant ($ps \leqslant 0.05$) increases in gene expression in the majority of the OLG/myelin genes (with the exception of MAG) in both the hippocampus and the white matter (MAG, CNP, PLP1, and MBP (Figure 6a and b; inset) and the pan probe for QKI (Figure 6a and b)). MBP was not affected in the white matter and MOBP was not affected in the hippocampus (not shown). MAG showed negligible gene expression ($p < 0.001$) in both brain regions of the MAG null mice. The gene expression of the majority of cell cycle genes was not affected. The mRNA levels of p57^{Kip2} were significantly

decreased in the hippocampus (Figure 6b), but not in the white matter of MAG null mice, suggesting that this decrease is unlikely to be associated with OLGs.

DISCUSSION

The studies described above were performed in the anterior cingulate cortex, the region where the most dramatic changes in the expression of myelin-specific markers were demonstrated previously in persons with SZ (Katsel *et al*, 2005b; Dracheva *et al*, 2006). Analysis of the microarray data from this region using the Ingenuity Pathway database revealed the consistent presence of canonical cell cycle pathways among the top networks and molecular functions affected in SZ (Figure 1). Correlation matrices (Table 3) between the mRNA levels of the top five affected cell cycle proteins and the levels of the cell-specific markers in persons with SZ and controls reveal two major findings. Firstly, the complex relationship between Cdk inhibitors and cyclins on one side, and neuronal or glial markers on the other, were significantly compromised in SZ relative to controls. Specifically, the relationships between cell cycle proteins and glial markers were only residually sustained and the relationships between cell cycle proteins and neuronal markers were generally absent. Secondly, strong statistically significant negative correlations between the levels of the measured neuronal and glial markers in the comparison group were absent in the SZ group. These findings suggest, that in the ACG of persons with SZ the normal relationships between neuronal and oligodendro-glial gene expression are dissociated from each other and that the changes in gene expression of cell cycle proteins in SZ are likely to be associated with postmitotic myelinating OLGs. It is noteworthy that, these observations generalized not only for PMP22 and SOX10, but for multiple other myelin/OLG specific markers (eg, CNP, MAG, PLP, MBP (data not shown)), which we assessed in additional exploratory analyses. The fact that GFAP, an astrocytic marker, also showed a significant correlation with cyclin D1
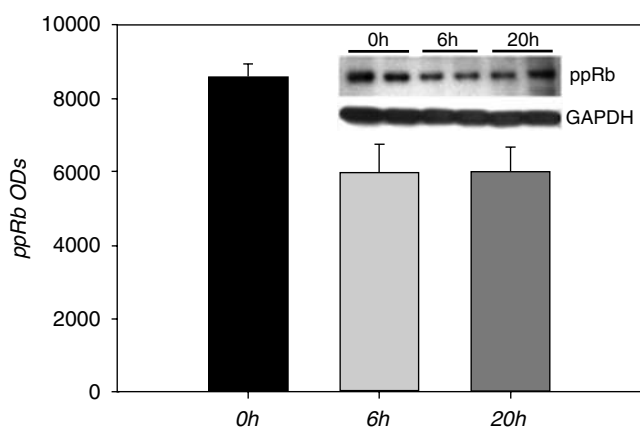

Figure 3 Stability of phosphorylated (S807/811) retinoblastoma protein—ppRb (S807/811) in the white matter of qk^{e5} mice measured by western blot. Brain samples from the same animal were either immediately frozen or stored for 6 and 20 h at room temperature to compare abundance of ppRb (S807/811). ppRb ODs—optical densities of ppRb normalized to the background. Data expressed as means ± SEM.
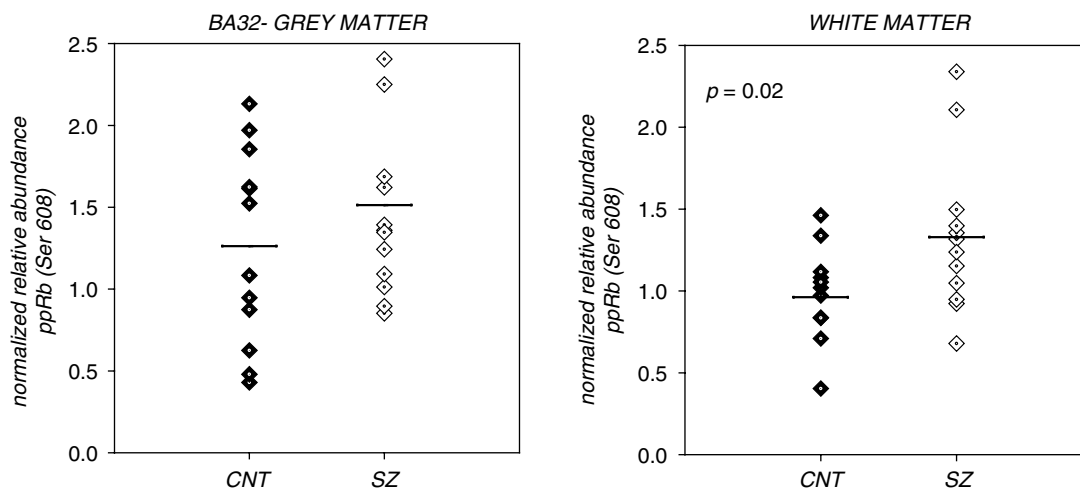

Figure 4 Relative abundance of phosphorylated (Ser608) retinoblastoma protein in the gray matter of ACG and the white matter of patients with SZs. Expression of ppRb (Ser608) was measured by western blot. Data expressed as means of ppRb (Ser608) ODs normalized to the underphosphorylated pRb and GAPDH and to the amount of total protein ($N = 12$/group). Plot displays the group means (horizontal line).
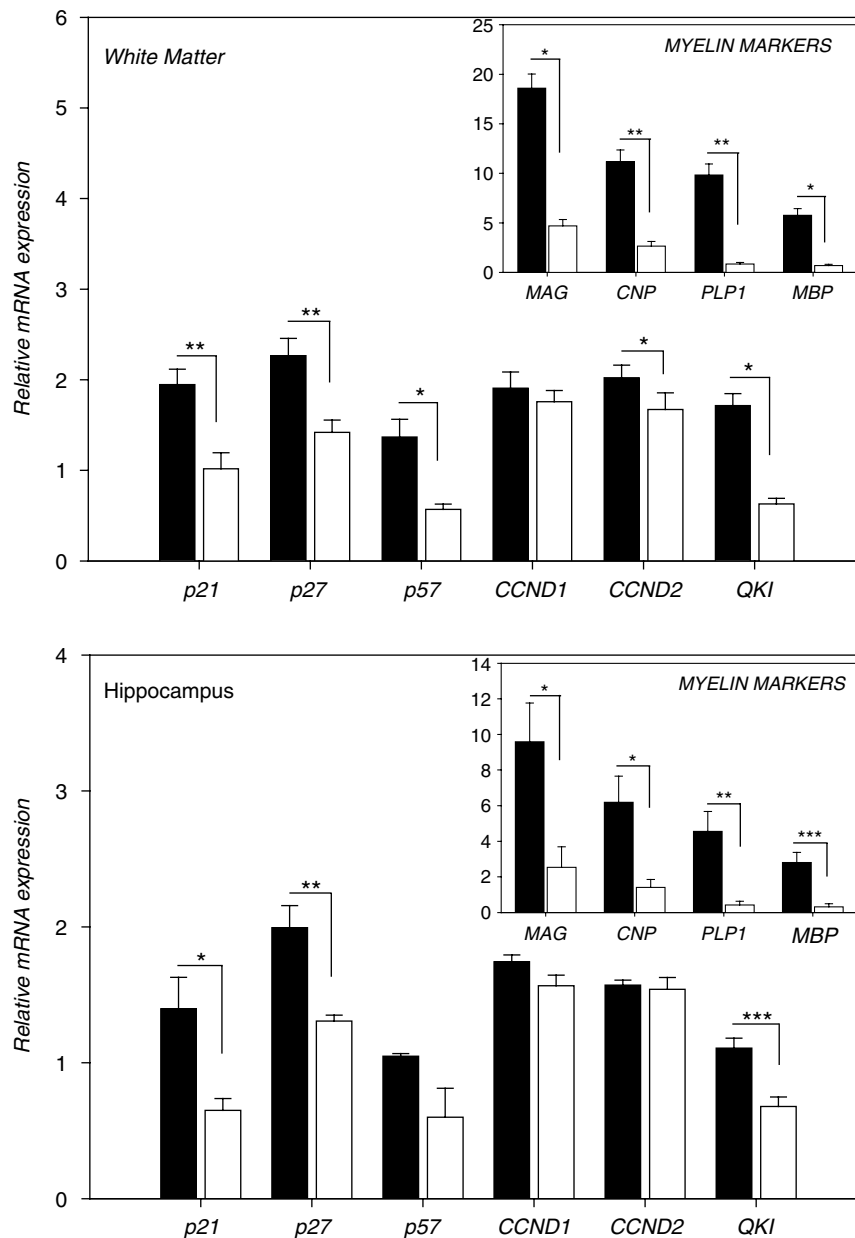
Figure 5 Relative mRNA expression of G1/S checkpoint genes and myelin proteins in the white matter and the hippocampus of quaking (qk^{e5}) mice. Gene expression was measured by qPCR. Data expressed as geometric means of individual expression values normalized to two housekeeping genes ± SEM. Inserts showed gene expression of myelin-specific proteins. Wild type (black bars) and qk^{e5} (white bars) mice ($N = 4$/group). *$ps < 0.05$, **$ps < 0.01$, ***$ps < 0.001$.

in SZ (Table 5) may also implicate the involvement of astrocytes. However, a recent study reported the existence of mixed phenotype myelin marker-positive glia that also expressed GFAP (Dyer et al, 2000). The population of these cells has been shown to be dramatically increased under different pathologic conditions. Another astrocyte marker, PEA15, 15 kDa, a phosphoprotein enriched in astrocytes, was not correlated (data not shown) with any of the tested genes, refuting the involvement of astrocytes.

Gene expression changes for four cell cycle proteins were validated by qPCR. We conditionally subdivided them into two groups by their time-dependent involvement in cell cycle activation: G1/S phase transition and G1/S checkpoint. The first group included the Cdk inhibitor, $p57^{Kip2}$ and

cyclin D1, which are the early regulators of the G1 phase entry and their mutually opposing activities are decisive for G1/S phase transition. The second group, the G1/S checkpoint genes, included TFDP1 and NPAT, the nuclear protein ataxia-telangiectasia locus. TFDP1 is a dimerization partner of the E2F transcription factor and when in complex with E2F, activates transcription of cell cycle proteins necessary for DNA replication and proliferation. NPAT is a primary substrate for cyclin E/Cdk2 complex and is essential for histone gene expression and S phase entry (Zhao et al, 2000; Gao et al, 2003). The changes observed in the identified cell cycle genes are particularly interesting because two of these genes, CCND1 and $p57^{Kip2}$, have been shown to be among the early regulated cell cycle genes in
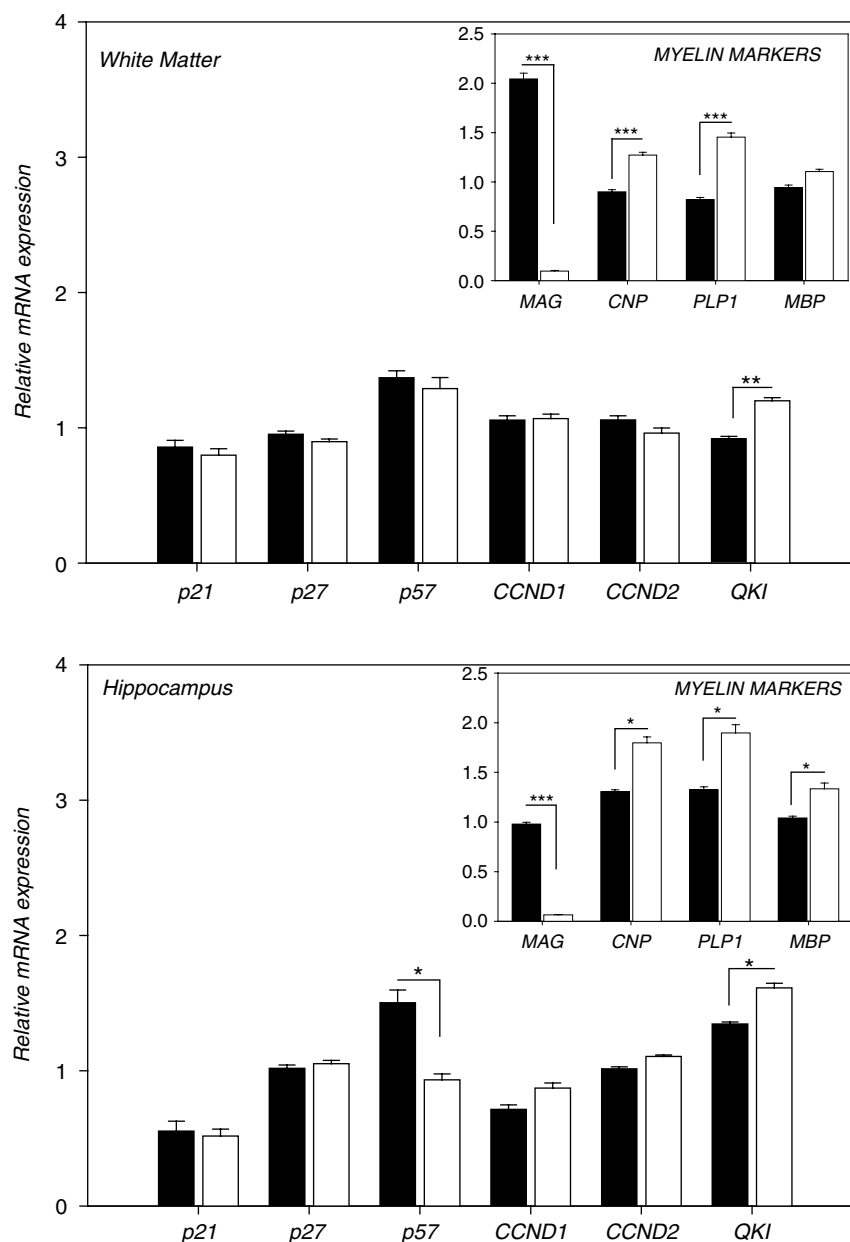
Figure 6 Relative mRNA expression of G1/S checkpoint genes and myelin proteins in the white matter and the hippocampus of MAG null mice. Gene expression was measured by qPCR. Data expressed as geometric means of individual expression values normalized to two housekeeping genes ± SEM. Inserts showed gene expression of myelin-specific proteins. Wild type (black bars) and MAG null (white bars) mice ($N = 8$/group). *$ps < 0.05$, **$ps < 0.01$, ***$ps < 0.001$.

OPCs after withdrawal of mitogen and exposure to thyroid hormones and thus may be central to OLG differentiation (Dugas et al, 2006, 2007).

Neuroleptic exposure is a confounding factor in post-mortem studies of SZ and therefore can contribute to the detected gene expression abnormalities of the cell cycle proteins. However, comparison of controls with the subgroup of SZ subjects who were free of anti-psychotic medication for 4 weeks or more prior to death suggests that the acute effects of neuroleptic treatment are an unlikely basis for the detected gene expression abnormalities. Although it can be argued that a few weeks, months or years of neuroleptic washout may not compensate for years of exposure to neuroleptics, this argument appears less

germane to cell cycle gene expression, which in theory, could be responsive to more short-term biological triggers. A recently published study also supports the data presented here (Table 6 and Figure 1) by suggesting that at least one antipsychotic drug, quetiapine, facilitates the development of OLGs rather than affecting them adversely (Xiao et al, 2007). However, the possibility of neuroleptic exposure confounds cannot be ruled out since it is possible that under some conditions, once cell cycle reentry has been triggered, continued exposure to the triggering mechanism(s) may not be obligatory (Yang et al, 2006; Herrup and Yang, 2007). In addition, a multiplicity of other environmental and nondisease-related factors, such as the possibility of environmental impoverishment, distinguishes
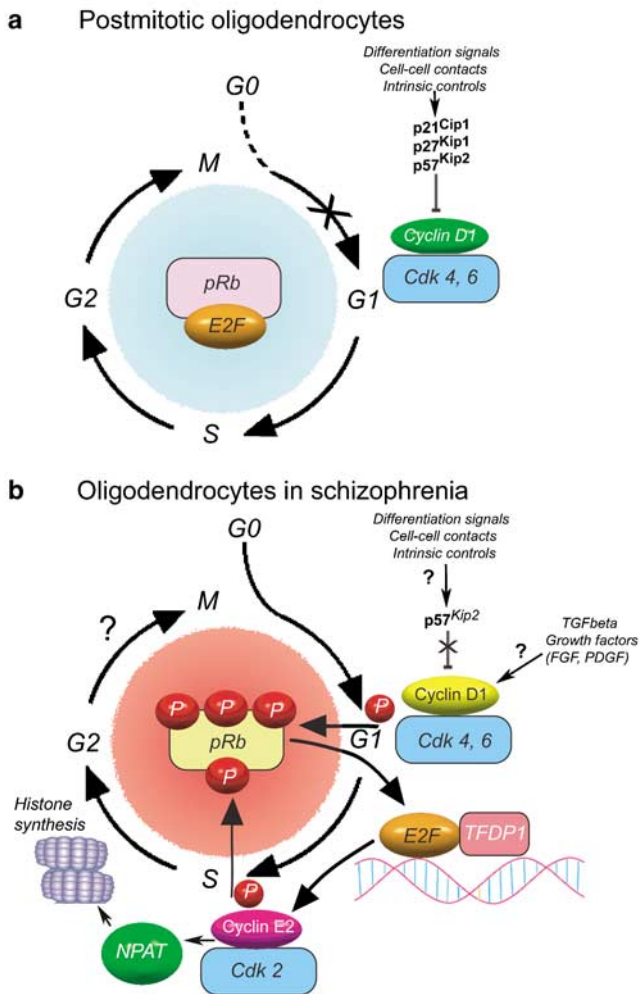
a Postmitotic oligodendrocytes

b Oligodendrocytes in schizophrenia

Figure 7 Hypothetical diagram of cell cycle re-entry in postmitotic oligodendrocytes in schizophrenia. (a) In normal postmitotic OLGs abundant expression of Cdk inhibitors: $p21^{Cip1}$, $p27^{Kip1}$, and $p57^{Kip2}$ maintain cell cycle arrest by inhibiting formation of cyclins D and E/Cdk2,4, and 6 complexes. Low activity of cyclins/CDK complexes sustains pRb in the underphosphorylated state and guarantees its cell cycle suppression activity. (b) In postmitotic OLGs in persons with SZ, gene expression of $p57^{Kip2}$ is decreased which relieves inhibition of Cdk/cyclin D complex formation. Activated cyclin D1/Cdk4 complexes carry out phosphorylation of pRb and subsequent liberation of E2F transcription factors. E2F in complex with TFDP1 initiates transcription of multiple cell cycle proteins, including cyclin E2. Activity of cyclin E2/Cdk2 complexes completes G1/S phase transition and initiates histone gene expression necessary for DNA replication to occur, via its substrate NPAT.

persons with SZ from the general population. The contribution of these extrinsic factors must be considered seriously in all neurobiological studies of SZ.

Myelin mutant mice were analyzed to determine whether they exhibited OPC/OLG-related cell cycle abnormalities similar to those observed in ACG in SZ subjects. Gene expression was compared in two myelin mutant animal models: quaking and MAG-null mice. Quaking mice, characterized by profound hypomyelination, and decreased gene expression of 10 myelin/OLG-specific proteins, showed significant downregulation in gene expression of Cip/Kip family of Cdk inhibitors in the white matter, and hippocampus (Figure 5) as well as frontal cortex (not shown). This observation suggests that OLG(s)-related cell

cycle abnormalities may underlie the myelin deficits in these mutant mice. The finding that gene expression of cyclin D2 was also decreased in the white matter of quaking mice was somewhat intriguing. This decrease, however, was not detected in the hippocampus or frontal cortex of quaking mice, suggesting that the CCND2 downregulation is OLG-specific and possibly regulated at least in part by the QKI proteins. Interestingly, it has been shown that the coding region of six different cyclin genes contain consensus-binding regions for the QKI proteins (Larocque et al, 2005).

MAG, on the other hand, is a structural myelin protein and its adaxonal localization is suggestive of its involvement in the interactions between axons and myelin sheaths (Arquint et al, 1987; Attia et al, 1989). MAG-deficient mice evidence multiple subtle defects, including delayed CNS myelination, multiple myelin wrappings, defective long-term maintenance of myelin in aged mice, altered morphology of axons, and behavioral defects (Li et al, 1994; Bartsch, 1996; Bartsch et al, 1997). In contrast to quaking mice, MAG knockout mice were characterized by elevated mRNA levels of most of the ten myelin/OLG-specific proteins (Figure 6, inset) without significant changes in gene expression of cell cycle genes in the white matter (Figure 6a). Overall, the studied gene expression profile of these two different myelin mutant animal models demonstrated that cell-cycle gene expression changes are not a necessary consequence of the reduced expression of oligodendrocyte-specific genes, such as MAG, but that genes that are known to modulate cell cycle activity during oligodendrocytes development (eg, QKI proteins) can significantly impair the expression of multiple myelin genes, including those that are affected in SZ. These observations suggest that cell cycle gene and protein abnormalities are not merely a consequence of the abnormal expression of myelin-associated genes. Taken together, these observations raise the possibility that global deficits in the expression of myelin-associated genes are likely to be a result of abnormalities in the expression of cell cycle genes and proteins. Clearly, this is not the only possible conclusion, but these results suggest that comparison of gene expression in animal models with specific gene expression defects may be a fruitful approach to the analysis of cause and effect relationships between myelin gene expression deficits and abnormalities in the expression of cell cycle genes.

The increased gene expression of cyclin D1 and the downregulation of $p57^{Kip2}$—the inhibitor of CCND1/Cdk4,6 complexes in ACG of subjects with SZ may be due to the re-entry of postmitotic OLGs into the G1 phase of the mitotic cell cycle. In the quiescent postmitotic state, pRbs act as checkpoint suppressors) for G1/S phase transition by entrapping E2F proteins, which are essential for transcription of multiple cyclins, CDKs, and enzymes involved in DNA replication. This proliferative/suppressive activity of the pRbs is relieved by the cyclin/Cdk complex-dependent phosphorylation of pRb at multiple serine/threonine sites. Hyperphosphorylated pRbs release E2F proteins and complete the transition from G1 to S phase of the mitotic cell cycle. Our data demonstrated a significant increase in the abundance of the ppRb protein in quaking mutant mice, which was consistent with the decreased gene expression of

major Cdk inhibitors in the OLGs of quaking mice. These findings further suggest that hypomyelination of the CNS may be the result of incomplete differentiation of OLG progenitors. Furthermore, the current findings of a significant increase in CCND/Cdk4-specific phosphorylation (Ser608) of pRb in the white matter of SZ subjects (Figure 4) provides additional evidence for the premise that SZ-associated changes in gene expression of cell cycle proteins are likely to occur in OLGs. Although the increase in ppRb in SZ was not as profound as that observed in quaking mice, a lesser increase in ppRb levels in SZ is consistent with the fact that myelin-associated gene expression deficits in SZ are far less profound than the nearly complete suppression of myelin-associated gene expression in quaking mice.

The current findings raise several questions: if the activation of cell cycle pathways takes place in SZ, what happens to the mitotically reactivated OLGs and what is the morphologic and molecular evidence supporting this reactivation? Cell cycle activation of postmitotic cells is tightly guarded by the checkpoint mechanism, which not only prevents cell proliferation but is also tightly coupled to apoptosis and eventual cell cycle-related death (Herrup and Yang, 2007). Therefore, at least two possibilities can exist for mitotically reactivated OLGs. The first possibility is that the initiation of apoptotic mechanisms would eventually lead to cell death and subsequent reduction of OLG densities in SZ. The second possibility is that apoptosis does not take place and mitotically reactivated OLGs continue their transition from G1 to other phases of the canonical cell cycle. This should eventually lead to mitosis and a subsequent increase in the proliferation rate of OLGs, suggesting increased number of OLGs in ACG of SZ subjects.

Our microarray data (Katsel *et al*, 2005b) from ACG and other brain regions of subjects with SZ indicate decreases in mRNA levels of many of the pro-apoptotic genes. Reports of similar findings from other gene expression studies in different brain regions of subjects with SZ (Benes *et al*, 2006) further substantiate the current data. Reduced DNA fragmentation (Benes *et al*, 2003) and lack of reduction in OLG density in the ACG in SZ (Segal *et al*, 2006) refute the concurrent activation of the apoptotic process in oligodendrocytes in SZ. In contrast, other research has shown a decrease in the number of glial cells in the ACG in subjects with SZ (Stark *et al*, 2004). Timing of typical apoptotic process (~12 h) predicts a rapid death for the affected cell population, which should result in devastating cell losses with disease progression. Imaging and postmortem morphometric studies do not support such a devastating loss of white matter and also argue against a persistent and profound apoptotic process in SZ. Alternatively, mitotically activated differentiated cells may persist in a transitional state between cell cycle re-entry and cell death. For example, it has been reported that cycling postmitotic but functionally deficient neurons (sometimes termed 'undead') can persist in the brains of animal models with neurodegenerative diseases for a long period of time (Yang *et al*, 2006).

Another possibility for mitotically reactivated OLGs is to complete the cell cycle, which culminates in cell division and ultimately increases the number of mitotically active cells. Such a mechanism has been posited to exist in the brains of aged non-human primates (Peters, 2002; Peters

and Sethares, 2003, 2004; Hinman *et al*, 2006). As such, another question that needs to be addressed is identifying the specific markers that distinguish these mitotically active cells. We (Hakak *et al*, 2001; Katsel *et al*, 2005b; Dracheva *et al*, 2006) and others (Tkachev *et al*, 2003; Aston *et al*, 2004) have previously reported decreases in gene expression in the majority of the late markers of OLG differentiation (Dugas *et al*, 2006), including MAG, MOG, MAL, TF, and TM4SF11 in multiple brain regions of SZ subjects. Microarray and qPCR data indicate that the gene expression of early markers of OLG differentiation (Hakak *et al*, 2001; Tkachev *et al*, 2003; Aston *et al*, 2004; Katsel *et al*, 2005b; Dracheva *et al*, 2006; Dugas *et al*, 2006), specifically, CNP, CLDN11, and CD9, was also significantly decreased in multiple brain regions, and PLP1 was decreased in ACG (microarray data, unpublished) and in PFC (Tkachev *et al*, 2003) in SZ. Gene expression of MBP was not changed in the current datasets, although others have demonstrated significant decreases in SZ (Tkachev *et al*, 2003). Therefore, it is unlikely that mitotically reactivated OLGs retain the ability to express these OLG-specific proteins. Nevertheless, it remains possible that mitotically reactivated oligodendrocytes are functionally deficient and express abnormally low levels of OLG-specific genes. This possibility can be addressed empirically in future studies.

Although to date, the signaling pathway(s) that induce cell cycle re-entry in OLGs remains unclear, one of many empirically testable hypotheses is schematized in Figure 7. This figure outlines a hypothetical sequence of events that is consistent with the data presented above. In postmitotic OLGs (Figure 7a), cell cycle activity is suppressed. Intrinsic control systems, maintain high levels of the Cip/Kip family of Cdk inhibitors (p21^{Cip1}, p27^{Kip1}, and p57^{Kip2}), which keep the formation of cyclin D/E- Cdk complexes under control, thus sustaining dephosphorylated pRb in the proliferation–suppression state. In SZ, postmitotic OLGs may undergo 'dedifferentiation' transformation (Figure 7b). Increased levels of cyclin D1 and reduced levels of p57^{Kip2}, resulting from elevated levels of mitogen or growth factors, or withdrawal of differentiation factors, promote formation of CCND1/Cdk4, six complexes, and increase phosphorylation of pRb and subsequent release of E2F transcription factor. E2F, in combination with TFDP1, initiate transcription of cyclin E2, and formation of CCNE2/Cdk2 complexes. The increased activity of CCNE2/Cdk2 complexes ensure phosphorylation of pRb and upregulation of NPAT, the protein necessary for DNA replication to occur, thus carrying out transition to the S phase. Whether DNA replication takes place and cells transition to the next phase(s) of mitotic cell cycle remain unanswered. Nevertheless, the detected profound abnormalities in the canonical cell cycle pathways in postmitotic OLGs are indicative of cell cycle re-entry, diverting OLGs from their postmitotic specialization and thus may be one of the bases for myelin-associated deficits in SZ.

DISCLOSURE/CONFLICT OF INTEREST

REFERENCES

Aberg K, Saetre P, Jareborg N, Jazin E (2006a). Human QKI, a potential regulator of mRNA expression of human oligodendrocyte-related genes involved in schizophrenia. *Proc Natl Acad Sci USA* 103: 7482–7487.

Aberg K, Saetre P, Lindholm E, Ekholm B, Pettersson U, Adolfsson R *et al* (2006b). Human QKI, a new candidate gene for schizophrenia involved in myelination. *Am J Med Genet B Neuropsychiatr Genet* 141: 84–90.

Arnold SE, Trojanowski JQ (1996). Recent advances in defining the neuropathology of schizophrenia. *Acta Neuropathol (Berl)* 92: 217–231.

Arquint M, Roder J, Chia LS, Down J, Wilkinson D, Bayley H *et al* (1987). Molecular-cloning and primary structure of myelin-associated glycoprotein. *Proc Natl Acad Sci USA* 84: 600–604.

Aston C, Jiang L, Sokolov BP (2004). Microarray analysis of postmortem temporal cortex from patients with schizophrenia. *J Neurosci Res* 77: 858–866.

Attia J, Tropak M, Johnson PW, Newerly-Abranow W, Pawson T, Roder JC *et al* (1989). Modulated adhesion: a proposal for the role of myelin-associated glycoprotein in myelin wrapping. *Clin Chem* 35: 717–720.

Bahn S, Jones PB (2003). Gene expression in schizophrenia and bipolar disorder. *Schizo Res* 60: 60.

Barta PE, Pearlson GD, Powers RE, Richards SS, Tune LE (1990). Auditory hallucinations and smaller superior temporal gyral volume in schizophrenia. *Am J Psychiatry* 147: 1457–1462.

Bartsch S, Montag D, Schachner M, Bartsch U (1997). Increased number of unmyelinated axons in optic nerves of adult mice deficient in the myelin-associated glycoprotein (MAG). *Br Res* 762: 231–234.

Bartsch U (1996). Myelination and axonal regeneration in the central nervous system of mice deficient in the myelin-associated glycoprotein. *J Neurocytol* 25: 303–313.

Bartzokis G, Nuechterlein KH, Lu PH, Gitlin M, Rogers S, Mintz J (2003). Dysregulated brain development in adult men with schizophrenia: a magnetic resonance imaging study. *Biol Psychiatry* 53: 412–421.

Baumann N, Pham-Dinh D (2001). Biology of oligodendrocyte and myelin in the mammalian central nervous system. *Physiol Rev* 81: 871–927.

Benes FM (1989). Myelination of cortical-hippocampal relays during late adolescence. *Schizophr Bull* 15: 585–593.

Benes FM (1999). Evidence for altered trisynaptic circuitry in schizophrenic hippocampus. *Biol Psychiatry* 46: 589–599.

Benes FM, Davidson J, Bird ED (1986). Quantitative cytoarchitectural studies of the cerebral cortex of schizophrenics. *Arch Gen Psychiatry* 43: 31–35.

Benes FM, Matzilevich D, Burke RE, Walsh J (2006). The expression of proapoptosis genes is increased in bipolar disorder, but not in schizophrenia. *Mol Psychiatry* 11: 241–251.

Benes FM, Turtle M, Khan Y, Farol P (1994). Myelination of a key relay zone in the hippocampal formation occurs in the human brain during childhood, adolescence, and adulthood. *Arch Gen Psychiatry* 51: 477–484.

Benes FM, Vincent SL, Todtenkopf M (2001). The density of pyramidal and nonpyramidal neurons in anterior cingulate cortex of schizophrenic and bipolar subjects. *Biol Psychiatry* 50: 395–406.

Benes FM, Walsh J, Bhattacharyya S, Sheth A, Berretta S (2003). DNA fragmentation decreased in schizophrenia but not bipolar disorder. *Arch Gen Psychiatry* 60: 359–364.

Benjamini Y, Hochberg Y (1995). Controlling the false discovery rate—a practical and powerful approach to multiple testing. *J R Soc Ser B (Methodol)* 57: 289–300.

Bolstad BM, Irizarry RA, Astrand M, Speed TP (2003). A comparison of normalization methods for high-density oligonucleotide array data based on variance and bias. *Bioinformatics* 19: 185–193.

Buchsbaum MS, Tang CY, Peled S, Gudbjartsson H, Lu D, Hazlett EA *et al* (1998). MRI white matter diffusion anisotropy and PET metabolic rate in schizophrenia. *NeuroReport* 9: 425–430.

Budhraja V, Spitznagel E, Schaiff WT, Sadovsky Y (2003). Incorporation of gene-specific variability improves expression analysis using high-density DNA microarrays. *BMC Biol* 1: 1.

Cotter D, Mackay D, Landau S, Kerwin R, Everall I (2001). Reduced glial cell density and neuronal size in the anterior cingulate cortex in major depressive disorder. *Arch Gen Psychiatry* 58: 545–553.

Davis KL, Mohs RC, Marin D, Purohit DP, Perl DP, Lantz M *et al* (1999). Cholinergic markers in elderly patients with early signs of Alzheimer disease. *JAMA* 281: 1401–1406.

Davis KL, Stewart DG, Friedman JI, Buchsbaum M, Harvey PD, Hof P *et al* (2003). White matter changes in schizophrenia: Evidence for myelin-related dysfunction. *Arc Gen Psychiatry* 60: 443–456.

Dracheva S, Davis KL, Chin B, Woo DA, Schmeidler J, Haroutunian V (2006). Myelin-associated mRNA and protein expression deficits in the anterior cingulate cortex and hippocampus in schizophrenia. *Neurobiol Dis* 79: 157–173.

Dracheva S, Marras SA, Elhakem SL, Kramer FR, Davis KL, Haroutunian V (2001). N-methyl-D-aspartic acid receptor expression in the dorsolateral prefrontal cortex of elderly patients with schizophrenia. *Am J Psychiatry* 158: 1400–1410.

Dracheva S, McGurk SR, Davis KL, Haroutunian V (2005). mRNA expression of AMPA receptors and AMPA receptor binding proteins in the cerebral cortex of of elderly schizophrenics. *J Neurosci Res* 79: 868–878.

Dugas JC, Ibrahim A, Barres BA (2007). A crucial role for p57Kip2 in the intracellular timer that controls oligodendrocyte differentiation. *J Neurosci* 27: 6185–6196.

Dugas JC, Tai YC, Speed TP, Ngai J, Barres BA (2006). Functional genomic analysis of oligodendrocyte differentiation. *J Neurosci* 26: 10967–10983.

Dyer CA, Kendler A, Jean-Guillaume D, Awatramani R, Lee A, Mason LM *et al* (2000). GFAP-positive and myelin marker-positive glia in normal and pathologic environments. *J Neurosci Res* 60: 412–426.

Flynn SW, Lang DJ, MacKay AL, Goghari V, Vavasour IM, Whittall KP *et al* (2003). Abnormalities of myelination in schizophrenia detected *in vivo* with MRI, and post-mortem with analysis of oligodendrocyte proteins. *Mol Psychiatry* 8: 811–820.

Foong J, Maier M, Barker GJ, Brocklehurst S, Miller DH, Ron MA (2000). *In vivo* investigation of white matter pathology in schizophrenia with magnetisation transfer imaging. *J Neurol Neurosurg Psychiatr* 68: 70–74.

Foong J, Symms MR, Barker GJ, Maier M, Woermann FG, Miller DH *et al* (2001). Neuropathological abnormalities in schizophrenia: evidence from magnetization transfer imaging. *Brain* 124: 882–892.

Franklin KBJ, Paxinos G (1997). *The Mouse Brain in Stereotaxic Coordinates*. Academic Press: New York.

Friston KJ, Frith CD (1995). Schizophrenia: a disconnection syndrome? *Clin Neurosci* 3: 89–97.

Gallo V, Ghiani CA (2000). Glutamate receptors in glia: new cells, new inputs and new functions. *Trends Pharmacol Sci* 21: 252–258.

Gao G, Bracken AP, Burkard K, Pasini D, Classon M, Attwooll C et al (2003). NPAT expression is regulated by E2F and is essential for cell cycle progression. *Mol Cell Biol* 23: 2821–2833.

Geng Y, Eaton EN, Picon M, Roberts JM, Lundberg AS, Gifford A et al (1996). Regulation of cyclin E transcription by E2Fs and retinoblastoma protein. *Oncogene* 12: 1173–1180.

Giedd JN, Blumenthal J, Jeffries NO, Castellanos FX, Liu H, Zijdenbos A et al (1999). Brain development during childhood and adolescence: a longitudinal MRI study. *Nat Neurosci* 2: 861–863.

Goldman-Rakic PS (1999). The physiological approach: functional architecture of working memory and disordered cognition in schizophrenia. *Biol Psychiatry* 46: 650–661.

Goldman-Rakic PS, Selemon LD (1997). Functional and anatomical aspects of prefrontal pathology in schizophrenia. *Schizophr Bull* 23: 437–458.

Hakak Y, Walker JR, Li C, Wong WH, Davis KL, Buxbaum JD et al (2001). Genome-wide expression analysis reveals dysregulation of myelination-related genes in chronic schizophrenia. *Proc Natl Acad Sci USA* 98: 4746–4751.

Haroutunian V, Davis KL (2000). Neuropathology of schizophrenia. In: Breier A, Tran PV, Herrera J, Bymaster F, Tollefson GD (eds). *Current Issues in the Psychopharmacology of Schizophrenia*. Williams and Wilkins: Baltimore. pp 57–70.

Haroutunian V, Davies PJ, Vianna C, Buxbaum JD, Purohit DP (2006a). Tau protein abnormalities associated with the progression of Alzheimer disease type dementia. *Neurobiol Aging* 28: 1–7.

Haroutunian V, Katsel P, Dracheva S, Davis KL (2006b). The human homolog of QKI gene affected in the severe dysmyelination 'quaking' mouse phenotype is downregulated in multiple brain regions in schizophrenia. *Am J Psychiat* 163: 1834–1837.

Haroutunian V, Katsel P, Schmeidler J (2007). Transcriptional vulnerability of brain regions in Alzheimer's disease and dementia. *Neurobiol Aging*, advance online publication; doi:10.1016/j.neurobiolaging.2007.07.021.

Haroutunian V, Perl DP, Purohit DP, Marin D, Khan K, Lantz M et al (1998). Regional distribution of neuritic plaques in the nondemented elderly and subjects with very mild Alzheimer disease. *Arch Neurol* 55: 1185–1191.

Haroutunian V, Purohit DP, Perl DP, Marin D, Khan K, Lantz M et al (1999). Neurofibrillary tangles in nondemented elderly subjects and mild Alzheimer disease. *Arch Neurol* 56: 713–718.

Harrison PJ (1999). The neuropathology of schizophrenia. A critical review of the data and their interpretation. *Brain* 122(Part 4): 593–624.

Herrup K, Yang Y (2007). Cell cycle regulation in the postmitotic neuron: oxymoron or new biology? *Nat Rev Neurosci* 8: 368–378.

Hinman JD, Peters A, Cabral H, Rosene DL, Hollander W, Rasband MN et al (2006). Age-related molecular reorganization at the node of Ranvier. *J Comp Neurol* 495: 351–362.

Hof PR, Haroutunian V, Friedrich Jr VL, Byne W, Buitron C, Perl DP et al (2003). Loss and altered spatial distribution of oligodendrocytes in the superior frontal gyrus in schizophrenia. *Biol Psychiatry* 53: 1075–1085.

Huttenlocher PR (1979). Synaptic density in human frontal cortex—developmental changes and effects of aging. *Brain Res* 163: 195–205.

Irizarry RA, Hobbs B, Collin F, Beazer-Barclay YD, Antonellis KJ, Scherf U et al (2003). Exploration, normalization, and summaries of high-density oligonucleotide array probe level data. *Biostatistics* 4: 249–264.

Iwamoto K, Bundo M, Yamada K, Takao H, Iwayama-Shigeno Y, Yoshikawa T et al (2005). DNA methylation status of SOX10 correlates with its downregulation and oligodendrocyte dysfunction in schizophrenia. *J Neurosci* 25: 5376–5381.

Katsel P, Davis KL, Gorman JM, Haroutunian V (2005a). Variations in differential gene expression patterns across multiple brain regions in schizophrenia. *Schizo Res* 77: 241–252.

Katsel P, Davis KL, Haroutunian V (2004). Large-scale microarray studies of gene expression in multiple regions of the brain in schizophrenia and Alzheimer's disease. *Int Rev Neurobiol* 63: 41–81.

Katsel P, Davis KL, Haroutunian V (2005b). Variations in myelin and oligodendrocyte-related gene expression across multiple brain regions: A gene ontology study. *Schizo Res* 79: 157–173.

Katsel P, Li C, Haroutunian V (2007). Gene expression alterations in the sphingolipid metabolism pathways during progression of dementia and Alzheimer's disease: a shift toward ceramide accumulation at the earliest recognizable stages of Alzheimer's disease? *Neurochem Res* 32: 845–856.

Katsel PL, Davis KL, Haroutunian V (2005c). Large-scale microarray studies of gene expression in multiple regions of the brain in schizophrenia and Alzheimer's disease. *Int Rev Neurobiol* 63: 41–82.

Kornhuber J, Schultz A, Wiltfang J, Meineke I, Gleiter CH, Zochling R et al (1999). Persistence of haloperidol in human brain tissue. *Am J Psychiatry* 156: 885–890.

Kovelman JA, Scheibel AB (1984). A neurohistological correlate of schizophrenia. *Biol Psychiatry* 19: 1601–1621.

Larocca JN, Rodriguez-Gabin AG (2002). Myelin biogenesis: vesicle transport in oligodendrocytes. *Neurochem Res* 27: 1313–1329.

Larocque D, Galarneau A, Liu HN, Scott M, Almazan G, Richard S (2005). Protection of p27(Kip1) mRNA by quaking RNA-binding proteins promotes oligodendrocyte differentiation. *Nat Neurosci* 8: 27–33.

Li C, Tropak MB, Gerlai R, Clapoff S, Abramow-Newerly W, Trapp B et al (1994). Myelination in the absence of myelin-associated glycoprotein. *Nature* 369: 747–750.

Lim KO, Hedehus M, Moseley M, de Crespigny A, Sullivan EV, Pfefferbaum A (1999). Compromised white matter tract integrity in schizophrenia inferred from diffusion tensor imaging. *Arch Gen psychiatry* 56: 367–374.

Liu Y, Wu Y, Lee JC, Xue H, Pevny LH, Kaprielian Z et al (2002). Oligodendrocyte and astrocyte development in rodents: an in situ and immunohistological analysis during embryonic development. *Glia* 40: 25–43.

Lundberg AS, Weinberg RA (1998). Functional inactivation of the retinoblastoma protein requires sequential modification by at least two distinct cyclin-cdk complexes. *Mol Cell Biol* 18: 753–761.

Mariani TJ, Budhraja V, Mecham BH, Gu CC, Watson MA, Sadovsky Y (2003). A variable fold change threshold determines significance for expression microarrays. *FASEB J* 17: 321–323.

Meyer-Lindenberg A, Poline JB, Kohn PD, Holt JL, Egan MF, Weinberger DR et al (2001). Evidence for abnormal cortical functional connectivity during working memory in schizophrenia. *Am J Psychiatry* 158: 1809–1817.

Mirra SS, Heyman A, McKeel D, Sumi SM, Crain BJ, Brownlee LM et al (1991). The consortium to establish a registry for Alzheimer's disease (CERAD). Part II. Standardization of the neuropathologic assessment of Alzheimer's disease. *Neurology* 41: 479–486.

Mitkus SN, Hyde TM, Vakkalanka R, Kolachana B, Weinberger DR, Kleinman JE et al (2008). Expression of oligodendrocyte-associated genes in dorsolateral prefrontal cortex of patients with schizophrenia. *Schizophr Res* 98: 129–138.

Miyakawa T, Sumiyoshi S, Deshimaru M, Suzuki T, Tomonari H (1972). Electron microscopic study on schizophrenia. Mechanism of pathological changes. *Acta Neuropathol (Berl)* **20**: 67–77.

Nikulina EM, Skrinskaya JA, Avgustinovich DF, Popova NK (1995). Dopaminergic brain system in the quaking mutant mouse. *Pharmacol Biochem Behav* **50**: 333–337.

Noveroske JK, Hardy R, Dapper JD, Vogel H, Justice MJ (2005). A new ENU-induced allele of mouse quaking causes severe CNS dysmyelination. *Mamm Genome* **16**: 672–682.

Pavlidis P, Lewis DP, Noble WS (2002). Exploring gene expression data with class scores. *Pac Symp Biocomput* **7**: 474–485.

Pavlidis P, Qin J, Arango V, Mann JJ, Sibille E (2004). Using the gene ontology for microarray data mining: a comparison of methods and application to age effects in human prefrontal cortex. *Neurochem Res* **29**: 1213–1222.

Peters A (2002). The effects of normal aging on myelin and nerve fibers: a review. *J Neurocytol* **31**: 581–593.

Peters A, Sethares C (2003). Is there remyelination during aging of the primate central nervous system? *J Comp Neurol* **460**: 238–254.

Peters A, Sethares C (2004). Oligodendrocytes, their progenitors and other neuroglial cells in the aging primate cerebral cortex. *Cereb Cortex* **14**: 995–1007.

Purohit DP, Perl DP, Haroutunian V, Powchik P, Davidson M, Davis KL (1998). Alzheimer's disease and related neurodegenerative diseases in elderly patients with schizophrenia: a postmortem neuropathologic study of 100 cases. *Arch Gen Psychiatry* **55**: 205–211.

Raedler TJ, Knable MB, Weinberger DR (1998). Schizophrenia as a developmental disorder of the cerebral cortex. *Curr Opin Neurobiol* **8**: 157–161.

Rajkowska G, Miguel-Hidalgo JJ, Makkos Z, Meltzer H, Overholser J, Stockmeier C (2002). Layer-specific reductions in GFAP-reactive astroglia in the dorsolateral prefrontal cortex in schizophrenia. *Schizophr Res* **57**: 127–138.

Rajkowska G, Selemon LD, Goldman-Rakic PS (1998). Neuronal and glial somal size in the prefrontal cortex: a postmortem morphometric study of schizophrenia and Huntington disease. *Arch Gen Psychiatry* **55**: 215–224.

Roy K, Murtie JC, El-Khodor BF, Edgar N, Sardi SP, Hooks BM *et al* (2007). Loss of erbB signaling in oligodendrocytes alters myelin and dopaminergic function, a potential mechanism for neuropsychiatric disorders. *Proc Natl Acad Sci USA* **104**: 8131–8136.

Segal D, Haroutunian V, Schmitz C, Hof P (2006). Spatial distribution and density of oligodendrocytes in the cingulum bundle is unaltered in schizophrenia. *Abstr Soc Neurosci*.

Selemon LD, Goldman-Rakic PS (1999). The reduced neuropil hypothesis: a circuit based model of schizophrenia. *Biol Psychiatry* **45**: 17–25.

Selemon LD, Rajkowska G (2003). Cellular pathology in the dorsolateral prefrontal cortex distinguishes schizophrenia from bipolar disorder. *Curr Mol Med* **3**: 427–436.

Selemon LD, Rajkowska G, Goldman-Rakic PS (1998). Elevated neuronal density in prefrontal area 46 in brains from schizophrenic patients: application of a three-dimensional, stereologic counting method. *J Comp Neurol* **392**: 402–412.

Stark AK, Uylings HB, Sanz-Arigita E, Pakkenberg B (2004). Glial cell loss in the anterior cingulate cortex, a subregion of the prefrontal cortex, in subjects with schizophrenia. *Am J Psychiatry* **161**: 882–888.

Stevens JR (1973). An anatomy of schizophrenia? *Arch Gen Psychiatry* **29**: 177–189.

Sugai T, Kawamura M, Iritani S, Araki K, Makifuchi T, Imai C *et al* (2004). Prefrontal abnormality of schizophrenia revealed by DNA microarray impact on glial and neurotrophic gene expression. *Ann N Y Acad Sci* **1025**: 84–91.

Tamminga CA, Vogel M, Gao X, Lahti AC, Holcomb HH (2000). The limbic cortex in schizophrenia: focus on the anterior cingulate. *Brain Res Brain Res Rev* **31**: 364–370.

Terry R, DeTeresa R, Hansen L (1987). Neocortical cell counts in normal human adult aging. *Ann Neurol* **21 No 6**: 530–539.

Tkachev D, Mimmack ML, Ryan MM, Wayland M, Freeman T, Jones PB *et al* (2003). Oligodendrocyte dysfunction in schizophrenia and bipolar disorder. *Lancet* **362**: 798–805.

Torrey EF, Peterson MR (1974). Schizophrenia and the limbic system. *Lancet* **2**: 942–946.

Uranova N, Orlovskaya D, Vikhreva O, Zimina I, Kolomeets N, Vostrikov V *et al* (2001). Electron microscopy of oligodendroglia in severe mental illness. *Brain Res Bull* **55**: 597–610.

Uranova NA, Vostrikov VM, Orlovskaya DD, Rachmanova VI (2004). Oligodendroglial density in the prefrontal cortex in schizophrenia and mood disorders: a study from the stanley neuropathology consortium. *Schizo Res* **67**: 269–275.

Vostrikov VM, Uranova NA, Orlovskaya DD (2007). Deficit of perineuronal oligodendrocytes in the prefrontal cortex in schizophrenia and mood disorders. *Schizophr Res* **94**: 273–280.

Weinberger DR (1995). Neurodevelopmental prespectives in schizophrenia. In: Bloom FE and Kupfer DJ (eds). *Psychopharmacology: The Fourth Generation of Progress*. Raven Press: New York. pp 1171–1184.

Weinberger DR (1999). Cell biology of the hippocampal formation in schizophrenia. *Biol Psychiatry* **45**: 395–402.

Weinberger DR, Lipska BK (1995). Cortical maldevelopment, antipsychotic drugs, and schizophrenia: a search for common ground. *Schizophr Res* **16**: 87–110.

Xiao L, Xu H, Zhang Y, Wei Z, He J, Jiang W *et al* (2007). Quetiapine facilitates oligodendrocyte development and prevents mice from myelin breakdown and behavioral changes. *Mol Psychiatry*, advance online publication 7 August 2007; doi:10.1038/sj.mp.4002064.

Yang Y, Varvel NH, Lamb BT, Herrup K (2006). Ectopic cell cycle events link human Alzheimer's disease and amyloid precursor protein transgenic mouse models. *J Neurosci* **26**: 775–784.

Zarkowska T, Mittnacht S (1997). Differential phosphorylation of the retinoblastoma protein by G1/S cyclin-dependent kinases. *J Biol Chem* **272**: 12738–12746.

Zeman W, Innes JRM (1963). *Craigie's Neuroanatomy of the Rat*. Academic Press: New York.

Zhao J, Kennedy BK, Lawrence BD, Barbie DA, Matera AG, Fletcher JA *et al* (2000). NPAT links cyclin E-Cdk2 to the regulation of replication-dependent histone gene transcription. *Genes Dev* **14**: 2283–2297.